AMPK deficiency induces DNA methylation and aggravates colorectal tumorigenesis in AOM/DSS mice

Xiaofei Sun
Washington State University
Qiyu Tian
Washington State University
Yansong Xue
Washington State University
Shima Bibi
Washington State University
Min Du
Washington State University
Meijun Zhu (meijun.zhu@wsu.edu)
Washington State University

Research

Keywords: AMPK, colorectal cancer, epigenetic modification, α-ketoglutarate

Posted Date: May 27th, 2020

DOI: https://doi.org/10.21203/rs.3.rs-30525/v1

AMPK deficiency induces DNA methylation and aggravates colorectal tumorigenesis in AOM/DSS mice

Xiaofei Sun[1,a], Qiyu Tian[2,a], Yansong Xue[1], Shima Bibi[1], Min Du[2] and Meijun Zhu[1,*]

[1]School of Food Science, Washington State University, Pullman, WA 99164, USA

[2]Department of Animal Science, Washington State University, Pullman, WA 99164, USA

*Correspondence to Dr. Meijun Zhu, School of Food Science, Washington State University, Pullman, WA 99164, USA; School of Food Science, University of Idaho, Moscow, ID 83844, USA; meijun.zhu@wsu.edu; (509) 335-4815

[a]Both authors contributed equally to this work.

Abstract

Background: The incidence of colorectal cancer (CRC) is closely related to metabolic diseases. AMP-activated protein kinase (AMPK) is known as a key metabolic regulator. Recently, the regulartory function of AMPK in the perspective of cancer metabolic reprogramming have attracted increasingly attention.

Methods: To assess the regulatory role of AMPK in colonic tumorigenesis, we cross-bred AMPKα1-floxed mice with Lgr5Cre mice to specifically knockout AMPK α1 gene in intestinal stem cells, where Lgr5 is expressed, and their derived epithelial cells. The wild-type and AMPK knockout mice were subjected to azoxymethane-induced and dextran sulfate sodium promoted (AOM/DSS) colitis-associated CRC induction. Mechanisms were examined in Caco-2 cells. Stable AMPK knockout cell line was selected using G418.

Results: AMPK deficiency caused colonic hyperproliferation and pathological features, which was associated with accelerated CRC development including the augmentation of tumor number, tumor size, and hyperplasia in the AOM/DSS mouse model. The aggravated colorectal tumorigenesis induced by AMPK ablation likely resulted from the alteration of metabolites, as indicated by the reduced production of α-ketoglutarate, an obligate substrate for ten-eleven translocation hydroxylases (TETs) mediated DNA demethylation, in colonic tissues. Consistent with reduced α-ketoglutarate, the content of isocitrate dehydrogenase 1 and the activity of TET1 were markably decreased in AMPK deficient mice, correlated with reduced metastasis inhibitors, *Adamts1* (A disintegrin and metalloproteinase with thrombospondin motif 1) and *Mal* (myelin and lymphocyte), as well as DNA hypermethylation of *Mal* and *Mgmt* (O-6-methylguanine-DNA methyltransferase) promotor regions. The mismatch repair (MMR) protein MLH1 or MSH2 levels

were downregulated in AMPK deficient Caco-2 cells. AMPK activiation inhibited hypermethylation in promoter regions of *Adamts1*, *Mal* and *p16ink4a* in Caco-2 cells.

Conclusions: AMPK deficiency limits α-ketoglutarate concentration and aggregates suppressive epigenetic modifications of antioncogenes in gut epithelial cells, increasing risk of colorectal tumorigenesis. Because AMPK activity is ameable to change, AMPK may serve as a molecular target for colorectal cancer prevention and therapeutic.

Keywords: AMPK, colorectal cancer, epigenetic modification, α-ketoglutarate

Background

Colorectal cancer (CRC) is the third leading cause of cancer death [1]. Epidemiological studies report that metabolic diseases render patients susceptible to CRC and related mortality [2], indicating a close relationship between metabolic disorders and the CRC incidence. Colonic tumorigenesis is an accumulative consequence of genetic and epigenetic alterations in colonic epithelium. Abnormalities in epigenetic changes such as DNA methylation and histone methylation, occur more frequently compared to genetic mutations [3]. More than half of human genes possess promoters with CpG islands, the dinucleotides region regulated by DNA methylation [4]. Aberrant methylation in the promoters of tumor suppressors or metastasis inhibitor genes leads to transcriptional silencing [4]. A disintegrin and metalloproteinase with thrombospondin motif 1 (*Adamts1*, anti-angiogenic gene), myelin and lymphocyte (*Mal*, T-cell differentiation gene) and O-6-methylguanine-DNA methyltransferase (*Mgmt*) are screened as CRC associated markers characterized with hypermethylation in the promoter regions [4-6]. The ten eleven translocation enzymes (TETs) catalyze the conversion of 5-methylcytosine (5mC) to 5-hydroxymethyl-cytosine (5hmC), an essential step for DNA demethylation. In cancer cells such as breast cancer [7], melanoma [8] and gastric cancer [9], the expression of TETs is suppressed, which correlates with hypermethylation of related anti-oncogenic genes.

Unlike normal colonic cells, CRC cells generate energy dependent on aerobic glycolysis instead of oxidative phosphorylation [10]. The downregulation of the tricarboxylic acid cycle and its intermediates, such as α-ketoglutarate, reprograms the metabolic microenvironment to assist tumor initiation and development [11]. Emerging evidence suggests that metabolic enzymes and their metabolites might mediate carcinogenesis epigenetically [12-14]. α-Ketoglutarate is an

obligate substrate for TETs-mediated DNA demethylation, linking metabolism to epigenetic modifications.

AMP-activated protein kinase (AMPK), a critical metabolic mediator, is a promising therapeutic target for intestinal diseases including CRC [15]. The inactivation of AMPK is associated with tumorigenesis in melanoma [16] and thyroid cancer [17], while the activation of AMPK could be a therapeutic target for preventing tumor development and progression in breast and hepatic cancers [18, 19]. AMPK ablation decreases α-Ketoglutarate generation and TETs activity, which attenuates brown adipogenesis and thermogenesis [20]. Inactivation of TETs and the related loss of hydroxymethylcytosine induce DNA hypermethylation and tumorigenesis in melanoma [8]. In combination, these studies suggest a key role of AMPK in bridging metabolism to epigenetic modifications and tumorigenesis.

Polyphenolic compounds such as quercetin [21], magnolol [22], and berberine [23] are known for their anti-CRC effects with concomitant AMPK activation. Conversely, epithelial specific AMPK knockout increases cell proliferation in AMPK VilCre mice [24]. However, the direct relationship between AMPK and colorectal tumorigenesis has not been examined. In this study, we generated AMPK transgenic mice, which specifically knockout AMPK in intestinal stem cells, and further examined the role of AMPK in metabolic alteration, epigenetic modification and colorectal tumorigenesis in an AOM/DSS induced-CRC mouse model, as well as in cultured epithelial Caco-2 cells with AMPK ectopic expression.

Materials and methods

Mouse strains

All animal studies were performed according to an approved protocol by the Institutional Animal Care and Use Committee (IACUC) at Washington State University. C57BL/6J mice were

purchased from Jackson Laboratory (Bar Harbor, ME). Mice with AMPKα1-floxed gene (Prkaa1$^{tm1.1Sjm}$/J, Stock#: 014141, Jackson Laboratory) were cross-bred with Lgr5Cre mice (B6.129P2-lgr5$^{tm1(cre/ERT2)Cle}$/J, Stock#: 008875, Jackson Laboratory). To obtain AMPK intestinal stem cell-specific knockout (AMPK KO) mice, the resulting crossbred AMPK$^{fl/fl}$Lgr5Cre female mice, aged 6-weeks, were injected intraperitoneally with tamoxifen (9 mg per 40 g of body weight, Sigma, St. Louis, MO) in sunflower oil (Sigma) for three consecutive days.

Two animal studies were conducted. In study one, ten AMPK KO mice and ten wild-type (WT) mice were euthanized at the age of 20 weeks, when the proliferation of intestinal stem cells in crypts become stable [25], to analyze effects of AMPK KO in epithelial stem cell proliferation. In study two, ten AMPK KO mice and ten WT mice were induced to develop CRC as described below and euthanized at the age of 30 weeks, to analyze effects of AMPK KO on CRC incidence.

AOM/DSS-induced colorectal cancer

Colorectal cancer was induced as previously described with modifications [26]. Ten AMPK KO mice and ten WT mice at the age of 15 weeks were injected intraperitoneally with azoxymethane (AOM, MRI Global Chemical, Kansas, Missouri; 10 mg/kg body weight). One week after AOM injection, mice were subjected to three cycles of dextran sulfate sodium (DSS, Millipore Corporation, Billerica, MA) induction. Each cycle is four weeks in length with one-week administration of 1% (w/v) DSS in drinking water and three weeks of regular drinking water; the disease activity index (DAI) scores were evaluated per criteria described in the supplementary information (SI)(Table S1) [24]. Mice were sacrificed by cervical dislocation at 15 weeks after first DSS exposure; additional two weeks of recovery allow mice to develop colorectal tumors [27]. One mouse in each group became lethargic during the last cycle of DSS administration and was euthanized/excluded from further analyses.

Tumor analysis and colon sample collection

On the day of necropsy, mice were anesthetized intraperitoneally with tribromoethanol (250 mg/kg body weight), followed by cervical dislocation. For mice with CRC induction, mouse colon was removed, flushed with PBS, and opened longitudinally. Colonic tissues were measured for length using the ruler on a dissecting board (Thermo Fisher Scientific, Waltham, MA) with a black cover, imaged with the virtual camera perpendicular to the colon midline. The imaged colonic tissue were used for analyzing adenomatous polyp numbers and diameters using Image J software [28]. Adenomatous polyp loads per mouse were calculated as the sum of diameters of all adenomatous polyps [26].

To assess tissue pathological changes, 0.5 cm distal colons close to anus were fixed in 4% formaldehyde for 6 hours, embedded in OCT medium. The remaining colonic tissues were then frozen in liquid nitrogen and stored at -80 °C for further biochemical analyses.

Histopathological analysis

The distal colons embedded in OCT medium were cryo-sectioned at 5-μm thickness, and stained with hematoxylin and eosin stain as previously reported [29]. The pathological changes, including depth of injury, severity of inflammation and crypt damage, of WT and AMPK KO mice without AOM/DSS treatment were blindly scored per criteria listed in the supplementary Table S2. The histopathological scores of AOM/DSS treated mice were evaluated blindly as previously described [30]. Inflammation, epithelial defect, crypt atrophy, hyperplasia, and hyperplasia area were considered histopathological parameters and were scored from 0 to 4 as described in in the supplementary Table S3.

Cell culture

The human colonic cell line Caco-2 cell was purchased from American Type Culture Collection (Manassas, VA, USA) and grown in Dulbecco's Modified Eagle's medium (DMEM) (Sigma), supplemented with 10% fetal bovine serum (GE, Fairfield, CT, USA) and 100 units/ml penicillin-streptomycin (Life Technologies, Carlsbad, CA, USA). Cells were cultured at 37 °C with 5% CO_2 in a humidified incubator. AMPK stable knockout colonic cell line was selected as previously described [24]. Briefly, Caco-2 cells were transfected eGFP and pAMPKα K45R mutant (K45R) plasmid (Addgene, Cambridge, MA). For plasmid transfection, Caco-2 cells were transfected with plasmids using the Neon Transfection System (Invitrogen, Carlsbad, CA, USA). Medium was changed 12 h post transfection, when 400 μg/ml G418 (Amresco, Solon, OH, USA) was added to the transfected cells for 7 days to enrich cells with transfection. Medium was changed every day.

Immunoblotting analysis

Frozen colonic tissues were powdered in liquid nitrogen. The protein extracts from powdered colonic tissues or Caco-2 cells were separated by 10% SDS-PAGE and transferred to nitrocellulose membrane [24]. Membranes were visualized using an Odyssey Infrared Imaging System (Li-Cor Biosciences, Lincoln, NE). Band density was normalized to β-actin. Antibodies against p-AMPK, AMPKα1, IDH1, MGMT, HDAC1 and MAL were purchased from Cell Signaling Technology (Danvers, MA). IRDye 680 goat anti-mouse secondary antibody and IRDye 800CW goat anti-rabbit secondary antibody were purchased from Li-Cor Biosciences (Lincoln, NE).

Immunofluorescent staining

Cryosections of mouse colon tissues were blocked in 5% goat serum at room temperature for 1 h, then incubated with anti-Ki67 (1:200, BioLegend, San Diego, CA) overnight at 4°C. Tissue sections were then incubated with goat anti-mouse Alexa Fluor 555 secondary antibody (1:1000, Cell Signaling Technology) at room temperature for 1 h. The intensity of fluorescence was

examined using EVOS FL fluorescence microscope (Life TechnologiesCarlsbad, CA, USA) [24]. For each mouse, three cross-sections were collected at 70-100 μm interval. Three images were obtained per section while avoiding areas with tumors. Positive Ki67 staining was quantified using Image J software.

Reverse-transcriptase (RT)-PCR and quantitative PCR

Total RNA was extracted from colonic tissues using TRIzol (Sigma). cDNA was synthesized using iScript cDNA Synthesis Kit (Bio-Rad, Hercules, CA). qPCRs were performed using SYBR Green supermixture (Bio-Rad) on CFX96 RT-PCR detection system (Bio-Rad). The primers listed in Table S4 were designed to cross two exons to prevent amplification of genomic DNA. β-Actin was used as an internal control, and the $2^{-\Delta\Delta Ct}$ method was used to calculate relative changes.

Ten-eleven translocation hydroxylases activity assay

The powdered colonic tissues (30 mg) were homogenized in 300μl of hypotonic buffer, followed 20 min-incubation on ice. After adding 20 μl of 10% NP40, the suspension was vortexed vigorously and centrifuged at 3,000 × *g* for 10 min at 4 ℃ to separate the nuclear portion from the cytoplasmic portion. The pellet was suspended in 50 μl of nuclear extraction buffer. After incubation on ice for 30 min while vortex, the suspension was centrifuged at 14, 000 × *g* for 30 min at 4 ℃. The supernatant was used for TET activity assay following the instruction of an epigenase 5mC-hydroxylase TET activity kit (EpiGenTEK, Farmingdale, NY). The detailed procedure is presented in the SI.

α-Ketoglutarate assays

Total α-ketoglutarate of powdered colonic tissues was measured following manufacturer's manual of an α-ketoglutarate assay kit (Sigma). The activity of metabolites was normalized to the total

protein content. Relative concentrations were calculated as the change in absorbance value relative to the WT group.

Hydroxymethyl-DNA and methylcytosine immunoprecipitation

Hydroxymethyl-DNA and methylcytosine immunoprecipitation (IP) was performed as previously described [20]. Isolated colonic genomic DNA (10 μg) from powdered colonic tissues or Caco-2 cells was diluted in 300 μl TE buffer and sonicated into 300-1000bp fragments, denatured then immediately cooled on ice bath, followed by adding 1/10 volume of 10× IP buffer, and antibody, which included 5-hydroxymethylcytosine (5hmC) antibody, 5-methylcytosine (5mC) antibody, or normal rabbit IgG (Cell Signaling Technology). The DNA-antibody complex was incubated overnight at 4 °C and pulled down with pre-blocked Pierce™ magnetic protein A/G beads (Thermo Scientific). The captured beads were washed three times with 1×IP buffer and re-suspended in 250 μl digestion buffer. Following treatment with proteinase K, DNA was purified using a ChIP DNA clean and concentrator kit (Zymo Research, Irvine, CA), which was subjected to quantitative PCR (qPCR) using primers listed in Table S4. The relative enrichment of 5hmC or 5mC was determined by $2^{-\Delta\Delta Ct}$, with ΔCt calculated as the change in Ct value relative to input DNA.

Statistical analyses

Statistical analyses were conducted as previously described [24]. Data are presented as mean ± standard error of the mean (SEM). Mean difference was separated by the non-parametric Mann-Whitney test. Statistical significance is considered when $P \leq 0.05$.

Results

AMPK deletion induces pathological lesion, enhances proliferation and inhibits α-ketoglutarate production in colonic tissue

To assess the regulatory role of AMPK in CRC, we cross-bred AMPKα1-floxed mice with Lgr5Cre mice to specifically knockout AMPK α1 gene in intestinal stem cells, where Lgr5 is expressed, inducing AMPKα1 knockout in these cells and their derived epithelial cells. AMPK ablation in epithelial cells alone resulted in a higher pathological score in colonic tissues (Fig. 1a, b), associated with decreased AMPK phosphorylation/activation in the colonic tissue (Fig. 1c). The remaining AMPK detected in AMPK ablated tissues was likely due to the presence of other tissues in addition to the epithelial layer. The tumorigenic effects of AMPK ablation might be partially due to the hyperproliferation, shown by increased Ki67 positive staining cells, caused by AMPK deletion in the colonic crypt (Fig. 1d, e). As an energy regulator, AMPK regulates energy metabolism and alters cellular production of metabolites [20]. AMPK deletion decreased α-ketoglutarate content in colonic tissues (Fig. 2a). Because α-ketoglutarate is a rate-limiting factor of TET-mediated DNA demethylation [31], the reduction in α-ketoglutarate content due to AMPK deletion should inhibit TET1 activity, which was confirmed (Fig. 2b). AMPK deficiency was further associated with the downregulated *Adamts1* and *Mal* contents (Fig. 2c, d), which might be a result of TET suppression (Fig. 2b).

AMPK deficiency aggravates colorectal tumorigenesis

Because abnormal proliferation and inflammation lead to tumor initiation, we further conducted a study to analyze CRC development in AMPK KO mice. To evaluate roles of AMPK on the tumor development in colon, WT and AMPK KO mice were subjected to AOM/DSS colitis-associated CRC induction (Fig. 3a). AMPK KO mice showed higher disease index scores as a sum of weight loss, gross bleeding and stool consistency, especially in the recovery period after each DSS cycle (Fig. 3b-e). DSS induces a much higher level of proinflammatory cytokines in distal colon compared to proximal part [32], resulting in the adenocarcinoma formation in the distal colon of

AOM/DSS mice [33]. Significant tumorigenesis was detected in the distal colon and spread to the mid-colon in AMPK KO mice (Fig. 4b-d), accompanied with decreased colon length (Fig. 4e). Histologically, AMPK inactivation (Fig. 5a) triggered polyp formation in the distal colon (Fig. 5b, c). Likewise, abrogating AMPK induced colitis and epithelial damages, suggested by the worsened pathological scores containing exacerbated inflammation, epithelial defects, crypt atrophy, enlarged hyperplasia and hyperplasia area (Fig. 5b). As expected, proliferative cells augmented in AMPK KO mice (Fig. 5d, e), consistent to what was observed in AMPK KO mice without AOM/DSS induction (Fig. 1d, e).

AMPK ablation-induced CRC is associated with decreased α-ketoglutarate production and TET activity in colonic tissues

Metabolic reprogramming is closely associated with tumorigenesis [34]. The mutation in isocitrate dehydrogenase 1 (IDH1), the critical metabolic enzyme catalyzing α-ketoglutarate formation, was discovered in patients with primary CRC [35]. Accordingly, IDH1 was downregulated in the colon of AMPK KO mice (Fig. 6a), as was its metabolic product, α-ketoglutarate (Fig. 6b). Those were associated with downregulation of metastasis inhibitors, *Adamts1* and *Mal,* and MGMT (Fig. 6c, d). TETs activity was further decreased (Fig. 6e), consistent with depleted 5hmC and enriched 5mC in the promoters of *Mgmt* and *Mal* genes (Fig. 6f, g).

Since AMPK inactivation promoted colorectal tumorigenesis through inducing epigenetic modifications especially the DNA methylation in AOM/DSS treated mice, we further generated an AMPK knockout colonic cell line using pAMPKα K45R plasmid. AMPK KO cells showed lower expression of Adamts1 at both mRNA and protein levels (Fig. 7a, b), consistent with lower levels of MAL protein (Fig. 7b). Downregulated IDH1 protein expression (Fig. 7c) in AMPK KO cells was associated with decreased DNA mismatch repair protein MLH1 and MSH2 (Fig. 7b).

Additionally, AMPK deletion decreased 5hmC abundance in the promoter regions of *Adamts1* and *Mal* genes (Fig 7d), while increased 5mC abundance in the promoters of tumor suppressor gene *p16ink4a* (Fig 7e). Data from in vitro Caco-2 study supported the previous AOM/DSS study in mice. Collectively, these results showed that AMPK dysfunction induces epigenetic modifications that accelerates tumorigenesis.

Discussion

AMPK deficiency promotes colorectal carcinogenesis

CRC is the second most common lethal cancer in the United States [36]. Emerging evidence indicates that cancer is associated with metabolic reprogramming [34]. A meta-analysis of 15 studies including more than 2 million diabetic patients found that diabetic patients are susceptible to incidences of CRC [2]. Obesity, one of the predominant risk factors for metabolic disorders, increased the tumor growth in xenograft mice injected with colon adenocarcinoma cancer cells [37].

Intestinal epithelial cells are constantly renewed with a turnover every 4-5 days, which requires energy for sustained cell proliferation and differentiation [38]. AMPK, a critical mediator maintaining energy homeostasis, coordinates cellular metabolism to balance energy demand and supply. As a metabolic checkpoint, AMPK determines whether the energy is adequate to proceed cell division. However, dysfunctional AMPK causes metabolic disorders, which facilitates carcinogenesis [39]. Activation of AMPK reduces lethality in CRC patients, while the inactivation of AMPK promotes tumor development [40].

Metformin, the anti-diabetic drug, is a well-known pharmacological activator of AMPK. Epidemiologically, the use of metformin for patients suffering from both diabetes and CRC is

associated with a reduced occurrence of cancer-related death [2]. Metformin suppressed the formation of aberrant crypt foci during early stage CRC after mice were intraperitoneally injected with AOM six times [41]. Polyp size in the small intestine of $Apc^{min/+}$ mice decreased after metformin treatment [42]. Furthermore, metformin attenuated DSS-induced acute colitis and ameliorated AOM/DSS-induced tumorigenesis in interleukin-10-deficiency mice [43]. Likewise, chronic administration of metformin in mice decelerates induction of pancreatic [44], breast [18], and lung cancers [45].

During intestinal development, the balance between epithelial proliferation and differentiation from intestinal stem cells is delicately controlled. The disturbance in this intricate balance could lead to the progression of CRC. Without AOM/DSS induction, we found that AMPK ablation augmented proliferative cells in crypts, providing a possible explanation for CRC initiation. *In vitro*, metformin and AICAR arrest the cell cycle and inhibit the proliferation of breast [18], hepatic [19], and prostate cancer cells [46]. In response to AOM/DSS induction, AMPK deficiency aggravated colorectal tumorigenesis as evidenced by increased adenocarcinoma number, size and hyperplasia in AOM/DSS-induced AMPK KO mice. Similarly, AMPK deficiency in the intestinal epithelium (AMPK VilCre mice) exaggerated DSS-induced colitis and histopathological changes [24].

Key metabolite deficiency due to AMPK KO induces epigenetic alterations associated with CRC

α-Ketoglutarate, prominent metabolites in the tricarboxylic acid cycle, collaboratively links metabolism to epigenetic modifications. Unlike normal epithelial cells, cancer cells obtain energy depending on glycolysis rather than oxidative phosphorylation, the so-called Warburg effect [47]. In rapidly proliferating cells, like cancer cells, AMPK acts as a master metabolic regulator to

activate tricarboxylic acid cycle and inhibit fatty acid synthesis [48, 49]. AMPK inactivation was accompanied by a reduction of gene expression in the citric acid cycle of PTEN deficient mice, contributing to hyperplasia and hyperproliferation in thyroid [17].

Aberrant DNA hypermethylation contributes to cancer cell growth and survival, while DNA demethylation of those specific genes leads to cell death and apoptosis [50]. DNA demethylation is coordinated by TETs, which requires α-Ketoglutarate as a co-factor [51]. TET proteins have recently been described as 5mC hydroxylases that catalyze iterative oxidation, producing 5-hydorxymethylcytosine (5hmC), 5-formylcytosine (5fC) and 5-carboxylcytosine (5caC) [52], which further undergoes DNA demethylation through base excision repair (BER) pathway [53]. In this study, AMPK deletion decreased the IDH1 level and its catalytic product, α-Ketoglutarate, as well as the activity of TET1, suggesting its bridging roles in metabolism and epigenetic modifications. Consistently, AMPK ablation reduced IDH2 activity and its catalytic product, α-Ketoglutarate, in brown adipose tissue, thus decreasing TET activity and blocking DNA demethylation [20]. However, in colorectal cancerous tissues, IDH1, not IDH2, was frequently decreased.

Aberrant methylation in the promoters of metastasis inhibitor genes leads to transcriptional silencing [4]. During stepwise tumorigenesis, methylation in the promoter regions of *Adamts1*and *Mal* is the biomarker for early detection of CRC [5]. We presented evidence that AMPK deficiency aggregated tumorigenesis and down-regulated MGMT and MAL in AMPK KO mice with AOM/DSS induction, which were associated with hypermethylation in the promoters of both *Mgmt* and *Mal*. $p16^{INK4a}$ is a tumor suppressor gene that regulates cellular proliferation, which is often lost due to DNA methylation or mutation [54]; its reduction due to AMPK ablation is consistent with the protective effect of AMPK in tumorigenesis. MGMT is a DNA repair protein

that returns O-6-methylguanine back to guanine, and its suppression leads to G:C to A:T transitions occurred in mutagenic DNA lesion [55]. Likewise, MGMT deficiency accounts for 40-90% of colorectal tumorigenesis [56, 57], and MGMT mutation increased tumor formation in AOM/DSS induced CRC mouse model [58]. The hypermethylation in the MGMT promoter silences its expression [59], which is closely related to the mutation in KRAS (a typical CRC oncogene) [60] and p53 (a typical CRC tumor suppressor) [61]. Similar to MGMT, mismatch repair (MMR) genes MLH1 and MSH2 are critically important for maintaining DNA from mutagenesis, and hereditary nonpolyposis colorectal cancer (HNPCC)/Lynch syndrome is associated with germline mutations in these genes [62]. Consistently, MSH2 and MLH1 were decreased in AMPK KO colonic cells.

In summary, AMPK ablation induces hyperproliferation and accelerates colorectal tumorigenesis, likely through inducing epigenetic modifications, which is associated with reduced IDH1 content and α-Ketoglutarate production, as well as decreased TET activity. These data deepen the current understanding about the link between the intracellular energy sensor, AMPK, and CRC. Given that AMPK is inhibited in many pathophysiological conditions such as obesity and diabetes, which are considered as risk factors for CRC, AMPK provides an amiable drug target for alleviating intestinal tumorigenesis. The wide availability of drugs triggering AMPK activation, such as metformin, adds translational value to our findings.

Acknowledgements

This work was financially supported by National Institutes of USDA-National Institute of Food and Agriculture (USDA-NIFA) (2018-67017-27517), and Washington State University Agricultural Research Center Emerging Research Issues Competitive Grant.

Conflict of Interest

The authors declare no conflict of interest.

Figure legend

Figure 1. AMPK deficiency increases proliferation and pathological scores in colonic tissue of mice. Wild-type (WT, □) and AMPK intestinal stem cell-specific knockout (AMPK KO, ■) mice were euthanized at the age of 20 weeks; the colonic tissues were used for analyses. (a) Representative hematoxylin and eosin staining of distal colonic tissues. The blue rectangle highlighted the area was enlarged in the right image. Scale bars are 400 μm. (b) Pathological scores, which are the sum of the depth of injury, the severity of inflammation and crypt damage. (c) Relative protein p-AMPK/AMPK ratio. (d) The percentage of Ki67-positive nuclei of the total nuclei counted using Image J. (e) Representative immunofluorescent staining images of Ki67 (red) and DAPI (blue) of the frozen colonic tissue section. Ki67 positive staining represents proliferating cells. Scale bars are 200 μm. Mean ± SEM, n = 8, *: $P < 0.05$; **: $P < 0.01$.

Figure 2. AMPK deletion suppresses colonic α-ketoglutarate production and TETs activity. Wild-type (WT, □) and AMPK intestinal stem cell-specific knockout (AMPK KO, ■) mice were euthanized at the age of 20 weeks, and the colonic tissues were used. (a) Relative α-ketoglutarate concentration. (b) The activity of ten-eleven translocation hydroxylases (TETs). (c) mRNA expression of *Adamts1* and *Mal*. (d) Relative protein contents of MAL. Mean ± SEM, n = 8, *: $P < 0.05$; **: $P < 0.01$.

Figure 3. AMPK ablation aggravates disease activity in an AOM/DSS-induced CRC mouse. (a) Experimental design of azoxymethane (AOM) and dextran sulfate sodium (DSS) induced colorectal cancer. Wild-type (WT) and AMPK intestinal stem cell-specific knockout (AMPK KO) mice at the age of 15 weeks were injected with AOM (10 mg/kg body weight) at the first day of experimental week 0 (W0). One-week after AOM injection, mice were subjected to 3 cycles of

DSS induction. In each cycle, 1.0 % (w/v) DSS was provided in drinking water for 7 days followed by a 3-week of recovery. (b) Disease activity index over time, which is the sum of body weight loss (c), fecal gross bleeding (d), and stool consistency (e). Mean ± SEM, n = 9.

Figure 4. AMPK knockout accelerates adenomatous polyp development in an AOM/DSS-induced mouse. Wild-type (WT, □) and AMPK intestinal stem cell-specific knockout (AMPK KO, ■) mice were induced colon tumor with azoxymethane and dextran sulfate sodium and euthanized at the age of 30 weeks. (a) The representative images of the longitudinally opened colon. (b) Adenomatous polyp number. (c) Average adenomatous polyp diameter. (d) Adenomatous polyp load per mouse. (e) Colon length. Mean ± SEM, n = 9, *: $P < 0.05$; **: $P < 0.01$.

Figure 5. AMPK deficiency accelerates colorectal tumorigenesis. Wild-type (WT, □) and AMPK intestinal stem cell-specific knockout (AMPK KO, ■) mice were induced colon tumorigenesis with azoxymethane and dextran sulfate sodium and euthanized at the age of 30 weeks. (a) Relative p-AMPK/AMPK in colonic tissue. (b) Histopathological scores of colonic tissues. (c) Representative hematoxylin and eosin staining of distal colonic tissues; the blue rectangle highlighted the area was enlarged in the right image. (d) Representative immunofluorescent staining images of Ki67 (red) and DAPI (blue) of the frozen colonic tissue section. Ki67 positive staining represents proliferating cells. Scale bars are 200 μm. (e) The percentage of Ki67-positive nuclei out of the total nuclei was counted using Image J. Mean ± SEM, n = 9, #: $P < 0.1$; *: $P < 0.05$; **: $P < 0.01$.

Figure 6. AMPK ablation inhibits colonic α-Ketoglutarate contents and TETs activity in AOM/DSS-induced mice. Wild-type (WT, □) and AMPK intestinal stem cell-specific knockout (AMPK KO, ■) mice induced colon tumors with azoxymethane and dextran sulfate sodium and euthanized at the age of 30 weeks. (a) Relative protein contents of IDH1 in colonic tissue. (b) Relative α-Ketoglutarate concentration. (c) The mRNA expression of *Adamts1* and *Mal*. (d) Relative protein contents of MAL and MGMT in colonic tissue. (e) The activity of ten-eleven translocation hydroxylases (TETs). (f) 5hmC and (g) 5mC modifications in the promoters of *Mgmt* and *Mal*. Mean ± SEM, n = 9, *: $P < 0.05$; **: $P < 0.01$.

Figure 7. AMPK prevents promoters hypermethylation in Caco-2 cell. □: Caco-2 cells were transfected with eGFP plasmid(WT); ■: Caco-2 cells were transfected with pAMPKα K45R plasmid (AMPK KO). (a) The mRNA expression of *Adamts1* and *Mal*. (b) Relative protein contents of MLH1, MSH2 and MAL. (c) Relative protein contents of IDH1. (d) 5hmC and (e) 5mC modifications in the promoters of *Adamst1*, *Mal*, *Mgmt* and *p16ink4a*. Mean ± SEM, n = 3, *: $P < 0.05$.

Figure. 8. Schematic diagram of mechanisms linking AMPK to epigenetic modifications of colorectal tumorigenesis. In an AOM/DSS induced-CRC mouse model, AMPK activation increases α-Ketoglutarate, which promotes TET-mediated DNA demethylation in the promoters of antioncogenic genes, suppressing/preventing colorectal carcinogenesis. AMPK: AMP-activated protein kinase; CRC: colorectal cancer; Mal: myelin and lymphocyte; Mgmt: O-6-methylguanine-DNA methyltransferase promotor regions; TETs: ten-eleven translocation hydroxylases

References

1. Siegel R, DeSantis C, Jemal A. Colorectal cancer statistics, 2014. CA: a cancer journal for clinicians. 2014, 64(2):104-17.
2. Larsson SC, Orsini N, Wolk A. Diabetes mellitus and risk of colorectal cancer: a meta-analysis. J Natl Cancer Inst. 2005, 97(22):1679-87.
3. Fearon ER. Molecular genetics of colorectal cancer. Annual Review of Pathology: Mechanisms of Disease. 2011, 6:479-507.
4. Kim MS, Lee J, Sidransky D. DNA methylation markers in colorectal cancer. Cancer Metastasis Rev. 2010, 29(1):181-206.
5. Ahlquist T, Lind GE, Costa VL, Meling GI, Vatn M, Hoff GS et al. Gene methylation profiles of normal mucosa, and benign and malignant colorectal tumors identify early onset markers. Mol Cancer. 2008, 7(1):94.
6. Li M, Gao F, Xia Y, Tang Y, Zhao W, Jin C et al. Filtrating colorectal cancer associated genes by integrated analyses of global DNA methylation and hydroxymethylation in cancer and normal tissue. Sci Rep. 2016, 6.
7. Liu C, Liu L, Chen X, Shen J, Shan J, Xu Y et al. Decrease of 5-hydroxymethylcytosine is associated with progression of hepatocellular carcinoma through downregulation of TET1. PloS one. 2013, 8(5):e62828.
8. Lian CG, Xu Y, Ceol C, Wu F, Larson A, Dresser K et al. Loss of 5-hydroxymethylcytosine is an epigenetic hallmark of melanoma. Cell. 2012, 150(6):1135-46.
9. Kudo Y, Tateishi K, Yamamoto K, Yamamoto S, Asaoka Y, Ijichi H et al. Loss of 5‐hydroxymethylcytosine is accompanied with malignant cellular transformation. Cancer Sci. 2012, 103(4):670-76.
10. Warburg O. On the origin of cancer cells. Science. 1956, 123(3191):309-14.
11. Yan H, Parsons DW, Jin G, McLendon R, Rasheed BA, Yuan W et al. IDH1 and IDH2 mutations in gliomas. N Engl J Med. 2009, 360(8):765-73.
12. Katada S, Imhof A, Sassone-Corsi P. Connecting threads: epigenetics and metabolism. Cell. 2012, 148(1):24-28.
13. Lu C, Thompson CB. Metabolic regulation of epigenetics. Cell Metab. 2012, 16(1):9-17.
14. Teperino R, Schoonjans K, Auwerx J. Histone methyl transferases and demethylases; can they link metabolism and transcription? Cell Metab. 2010, 12(4):321-27.
15. Sun X, Zhu M-J. AMP-activated protein kinase: a therapeutic target in intestinal diseases. Open Biol. 2017, 7(8):170104.
16. Zheng B, Jeong JH, Asara JM, Yuan Y-Y, Granter SR, Chin L et al. Oncogenic B-RAF negatively regulates the tumor suppressor LKB1 to promote melanoma cell proliferation. Mol cell. 2009, 33(2):237-47.
17. Arciuch VGA, Russo MA, Kang KS, Di Cristofano A. Inhibition of AMPK and Krebs cycle gene expression drives metabolic remodeling of Pten-deficient preneoplastic thyroid cells. Cancer Res. 2013, 73(17):5459-72.
18. Zakikhani M, Dowling R, Fantus IG, Sonenberg N, Pollak M. Metformin is an AMP kinase–dependent growth inhibitor for breast cancer cells. Cancer Res. 2006, 66(21):10269-73.
19. Imamura K, Ogura T, Kishimoto A, Kaminishi M, Esumi H. Cell cycle regulation via p53 phosphorylation by a 5′-AMP activated protein kinase activator, 5-

aminoimidazole-4-carboxamide-1-β-D-ribofuranoside, in a human hepatocellular carcinoma cell line. Biochem Bioph Res Co. 2001, 287(2):562-67.
20. Yang Q, Liang X, Sun X, Zhang L, Fu X, Rogers CJ et al. AMPK/α-ketoglutarate axis dynamically mediates DNA demethylation in the Prdm16 promoter and brown adipogenesis. Cell Metab. 2016, 24(4):542-54.
21. Lee Y-K, Park SY, Kim Y-M, Lee WS, Park OJ. AMP kinase/cyclooxygenase-2 pathway regulates proliferation and apoptosis of cancer cells treated with quercetin. Exp Mol Med. 2009, 41(3):201-07.
22. Park JB, Lee MS, Cha EY, Lee JS, Sul JY, Song IS et al. Magnolol-induced apoptosis in HCT-116 colon cancer cells is associated with the AMP-activated protein kinase signaling pathway. Biol Pharm Bull. 2012, 35(9):1614-20.
23. Li W, Hua B, Saud SM, Lin H, Hou W, Matter MS et al. Berberine regulates AMP‐activated protein kinase signaling pathways and inhibits colon tumorigenesis in mice. Mol Carcinogenesis. 2015, 54(10):1096-109.
24. Sun X, Yang Q, Rogers CJ, Du M, Zhu M-J. AMPK improves gut epithelial differentiation and barrier function via regulating Cdx2 expression. Cell Death Differ. 2017, 24(5):819-31.
25. Mandir N, FitzGerald AJ, Goodlad RA. Differences in the effects of age on intestinal proliferation, crypt fission and apoptosis on the small intestine and the colon of the rat. Int J Clin Exp Pathol. 2005, 86(2):125-30.
26. Neufert C, Becker C, Neurath MF. An inducible mouse model of colon carcinogenesis for the analysis of sporadic and inflammation-driven tumor progression. Nat Protoc. 2007, 2(8):1998-2004.
27. Becker C, Fantini M, Wirtz S, Nikolaev A, Kiesslich R, Lehr H et al. In vivo imaging of colitis and colon cancer development in mice using high resolution chromoendoscopy. Gut. 2005, 54(7):950-54.
28. Abràmoff MD, Magalhães PJ, Ram SJ. Image processing with ImageJ. Biophotonics Int. 2004, 11(7):36-42.
29. Kang Y, Xue Y, Du M, Zhu M-J. Preventive effects of Goji berry on dextran-sulfate-sodium-induced colitis in mice. J Nutr Biochem. 2017, 40:70-76.
30. Meira LB, Bugni JM, Green SL, Lee C-W, Pang B, Borenshtein D et al. DNA damage induced by chronic inflammation contributes to colon carcinogenesis in mice. J Clin Invest. 2008, 118(7):2516-25.
31. Yang Q, Liang X, Sun X, Zhang L, Fu X, Rogers CJ et al. AMPK/alpha-ketoglutarate axis dynamically mediates DNA demethylation in the *Prdm16* promoter and brown adipogenesis. Cell Metab. 2016, 24(4):542-54.
32. Yan Y, Kolachala V, Dalmasso G, Nguyen H, Laroui H, Sitaraman SV et al. Temporal and spatial analysis of clinical and molecular parameters in dextran sodium sulfate induced colitis. PloS one. 2009, 4(6):e6073.
33. Parang B, Barrett CW, Williams CS: AOM/DSS model of colitis-associated cancer. In: Gastrointestinal Physiology and Diseases. edn.: Springer; 2016: 297-307.
34. Ward PS, Thompson CB. Metabolic reprogramming: a cancer hallmark even warburg did not anticipate. Cancer Cell. 2012, 21(3):297-308.
35. Sjöblom T, Jones S, Wood LD, Parsons DW, Lin J, Barber TD et al. The consensus coding sequences of human breast and colorectal cancers. science. 2006, 314(5797):268-74.

36. Siegel RL, Miller KD, Jemal A. Cancer statistics, 2016. CA: a cancer journal for clinicians. 2016, 66(1):7-30.
37. Yakar S, Nunez NP, Pennisi P, Brodt P, Sun H, Fallavollita L et al. Increased tumor growth in mice with diet-induced obesity: impact of ovarian hormones. Endocrinology. 2006, 147(12):5826-34.
38. Van der Flier LG, Clevers H. Stem cells, self-renewal, and differentiation in the intestinal epithelium. Annu Rev Physiol. 2009, 71:241-60.
39. Fogarty S, Hardie D. Development of protein kinase activators: AMPK as a target in metabolic disorders and cancer. Biochim Biophys Acta, Proteins Proteomics. 2010, 1804(3):581-91.
40. Garrett C, Hassabo H, Bhadkamkar N, Wen S, Baladandayuthapani V, Kee B et al. Survival advantage observed with the use of metformin in patients with type II diabetes and colorectal cancer. Br J Cancer. 2012, 106(8):1374-78.
41. Hosono K, Endo H, Takahashi H, Sugiyama M, Uchiyama T, Suzuki K et al. Metformin suppresses azoxymethane‐induced colorectal aberrant crypt foci by activating AMP‐activated protein kinase. Mol Carcinogenesis. 2010, 49(7):662-71.
42. Tomimoto A, Endo H, Sugiyama M, Fujisawa T, Hosono K, Takahashi H et al. Metformin suppresses intestinal polyp growth in ApcMin/+ mice. Cancer Sci. 2008, 99(11):2136-41.
43. Koh SJ, Kim JM, Kim IK, Ko SH, Kim JS. Anti‐inflammatory mechanism of metformin and its effects in intestinal inflammation and colitis‐associated colon cancer. J Gastroenterol Hepatol. 2014, 29(3):502-10.
44. Schneider MB, Matsuzaki H, Haorah J, Ulrich A, Standop J, Ding XZ et al. Prevention of pancreatic cancer induction in hamsters by metformin. Gastroenterology. 2001, 120(5):1263-70.
45. Memmott RM, Mercado JR, Maier CR, Kawabata S, Fox SD, Dennis PA. Metformin prevents tobacco carcinogen–induced lung tumorigenesis. Cancer Prev Res. 2010, 3(9):1066-76.
46. Sahra IB, Laurent K, Loubat A, Giorgetti-Peraldi S, Colosetti P, Auberger P et al. The antidiabetic drug metformin exerts an antitumoral effect in vitro and in vivo through a decrease of cyclin D1 level. Oncogene. 2008, 27(25):3576-86.
47. Seyfried TN, Flores RE, Poff AM, D'Agostino DP. Cancer as a metabolic disease: implications for novel therapeutics. Carcinogenesis. 2014, 35(3):515-27.
48. Hardie DG. AMP-activated protein kinase—an energy sensor that regulates all aspects of cell function. Genes Dev. 2011, 25(18):1895-908.
49. Agathocleous M, Harris WA. Metabolism in physiological cell proliferation and differentiation. Trends Cell Biol. 2013, 23(10):484-92.
50. Weisenberger D, Liang G, Lenz H. DNA methylation aberrancies delineate clinically distinct subsets of colorectal cancer and provide novel targets for epigenetic therapies. Oncogene. 2018, 37(5):566.
51. Prensner JR, Chinnaiyan AM. Metabolism unhinged: IDH mutations in cancer. Nat Med. 2011, 17(3):291.
52. Kohli RM, Zhang Y. TET enzymes, TDG and the dynamics of DNA demethylation. Nature. 2013, 502(7472):472.
53. Cimmino L, Abdel-Wahab O, Levine RL, Aifantis I. TET family proteins and their role in stem cell differentiation and transformation. Cell Stem Cell. 2011, 9(3):193-204.

54. LaPak KM, Burd CE. The molecular balancing act of p16INK4a in cancer and aging. Mol Cancer Res. 2014, 12(2):167-83.
55. Shen L, Kondo Y, Rosner GL, Xiao L, Hernandez NS, Vilaythong J et al. MGMT promoter methylation and field defect in sporadic colorectal cancer. J Natl Cancer Inst. 2005, 97(18):1330-38.
56. Wong JJL, Hawkins NJ, Ward RL. Colorectal cancer: a model for epigenetic tumorigenesis. Gut. 2007, 56(1):140-48.
57. Mokarram P, Zamani M, Kavousipour S, Naghibalhossaini F, Irajie C, Sarabi MM et al. Different patterns of DNA methylation of the two distinct O6-methylguanine-DNA methyltransferase (O6-MGMT) promoter regions in colorectal cancer. Mol Biol Rep. 2013, 40(5):3851-57.
58. Fahrer J, Kaina B. O 6-methylguanine-DNA methyltransferase in the defense against N-nitroso compounds and colorectal cancer. Carcinogenesis. 2013, 34(11):2435-42.
59. Halford S, Rowan A, Sawyer E, Talbot I, Tomlinson I. O6-methylguanine methyltransferase in colorectal cancers: detection of mutations, loss of expression, and weak association with G: C> A: T transitions. Gut. 2005, 54(6):797-802.
60. Esteller M, Toyota M, Sanchez-Cespedes M, Capella G, Peinado MA, Watkins DN et al. Inactivation of the DNA repair gene O6-methylguanine-DNA methyltransferase by promoter hypermethylation is associated with G to A mutations in K-ras in colorectal tumorigenesis. Cancer Res. 2000, 60(9):2368-71.
61. Esteller M, Risques R-A, Toyota M, Capella G, Moreno V, Peinado MA et al. Promoter hypermethylation of the DNA repair gene O6-methylguanine-DNA methyltransferase is associated with the presence of G: C to A: T transition mutations in p53 in human colorectal tumorigenesis. Cancer Res. 2001, 61(12):4689-92.
62. Martin SA, McCabe N, Mullarkey M, Cummins R, Burgess DJ, Nakabeppu Y et al. DNA polymerases as potential therapeutic targets for cancers deficient in the DNA mismatch repair proteins MSH2 or MLH1. Cancer Cell. 2010, 17(3):235-48.

Figures

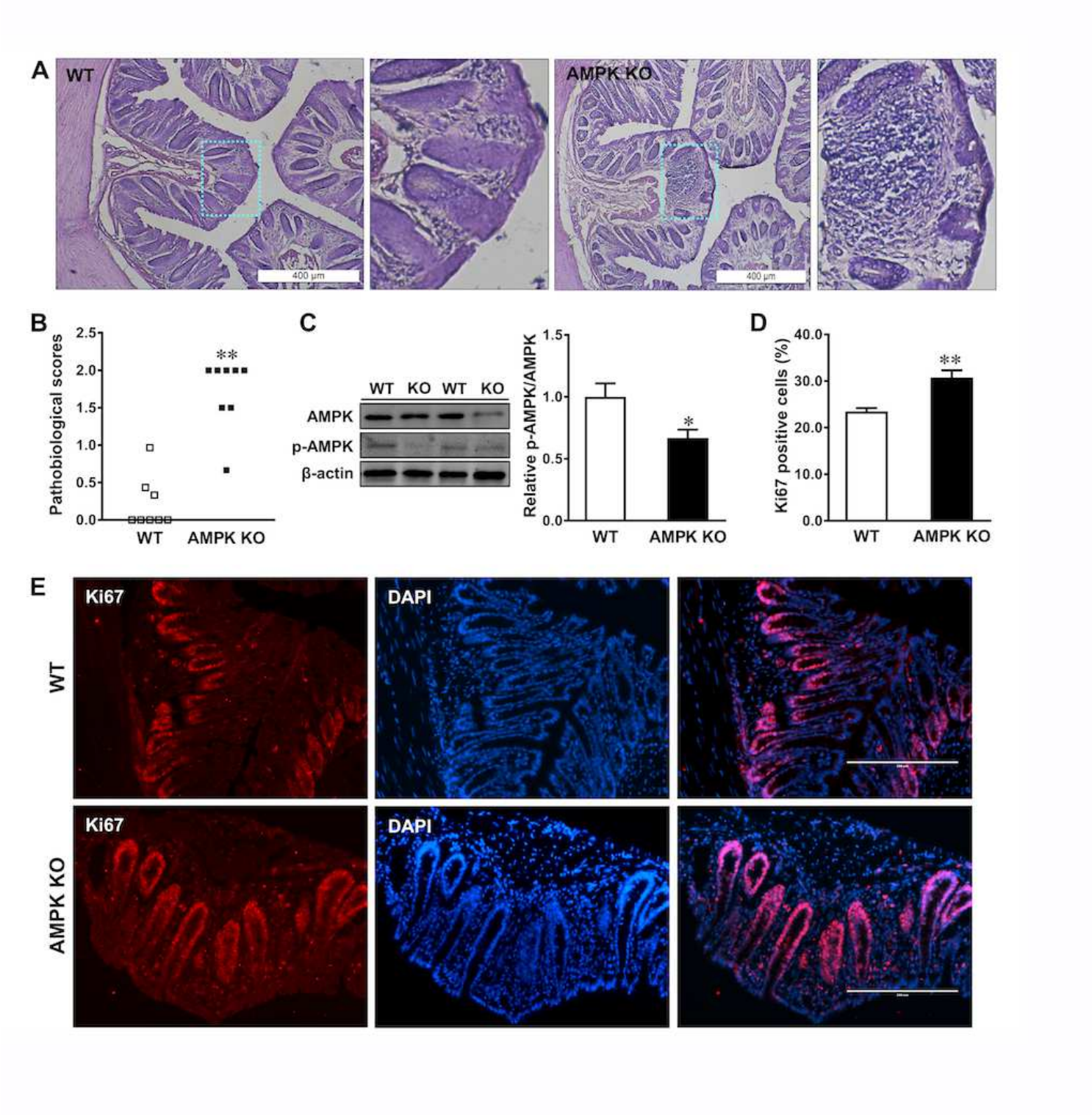

Figure 1

AMPK deficiency increases proliferation and pathological scores in colonic tissue of mice. Wild-type (WT, □) and AMPK intestinal stem cell-specific knockout (AMPK KO, □) mice were euthanized at the age of 20 weeks; the colonic tissues were used for analyses. (a) Representative hematoxylin and eosin staining of

distal colonic tissues. The blue rectangle highlighted the area was enlarged in the right image. Scale bars are 400 μm. (b) Pathological scores, which are the sum of the depth of injury, the severity of inflammation and crypt damage. (c) Relative protein p-AMPK/AMPK ratio. (d) The percentage of Ki67-positive nuclei of the total nuclei counted using Image J. (e) Representative immunofluorescent staining images of Ki67 (red) and DAPI (blue) of the frozen colonic tissue section. Ki67 positive staining represents proliferating cells. Scale bars are 200 μm. Mean ± SEM, n = 8, *: P < 0.05; **: P < 0.01.

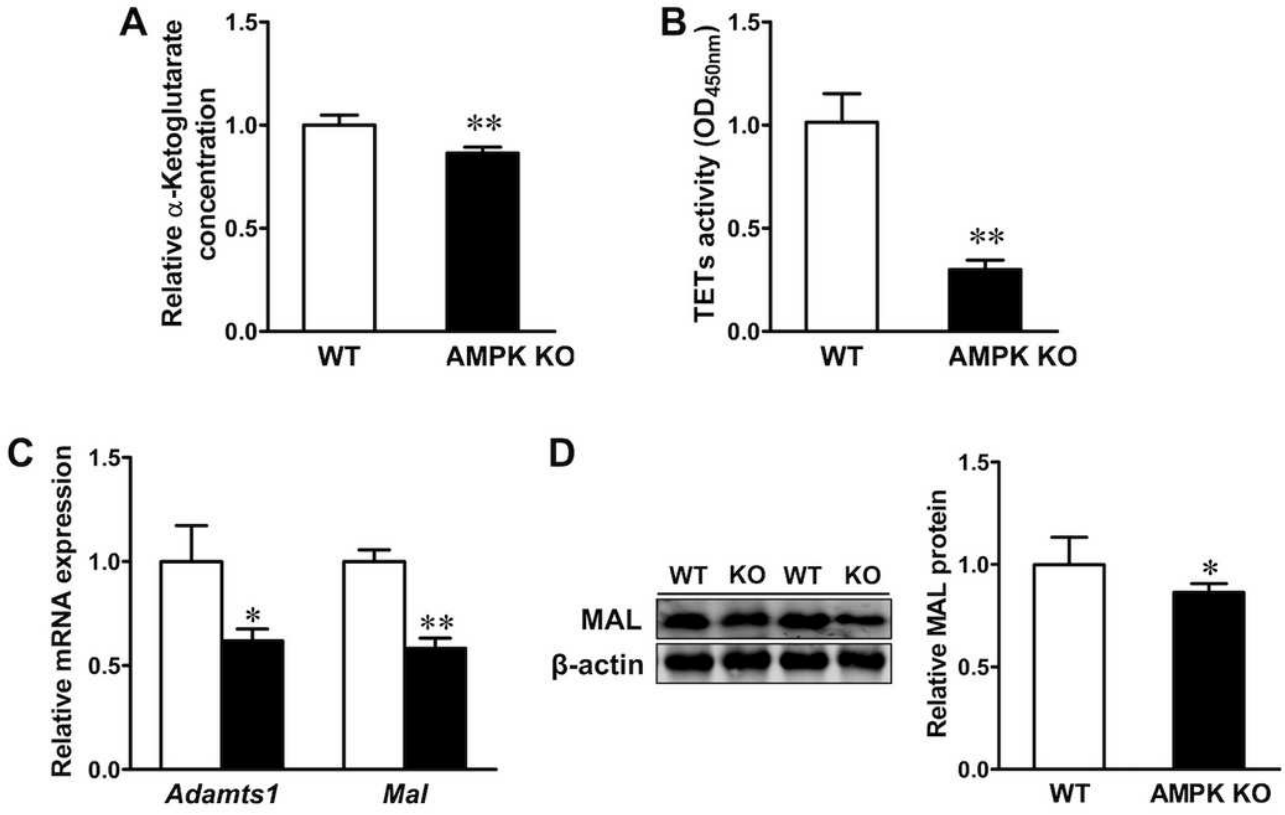

Figure 2

AMPK deletion suppresses colonic α-ketoglutarate production and TETs activity. Wild-type (WT, □) and AMPK intestinal stem cell-specific knockout (AMPK KO, ■) mice were euthanized at the age of 20 weeks, and the colonic tissues were used. (a) Relative α-ketoglutarate concentration. (b) The activity of ten-eleven translocation hydroxylases (TETs). (c) mRNA expression of Adamts1 and Mal. (d) Relative protein contents of MAL. Mean ± SEM, n = 8, *: P < 0.05; **: P < 0.01.

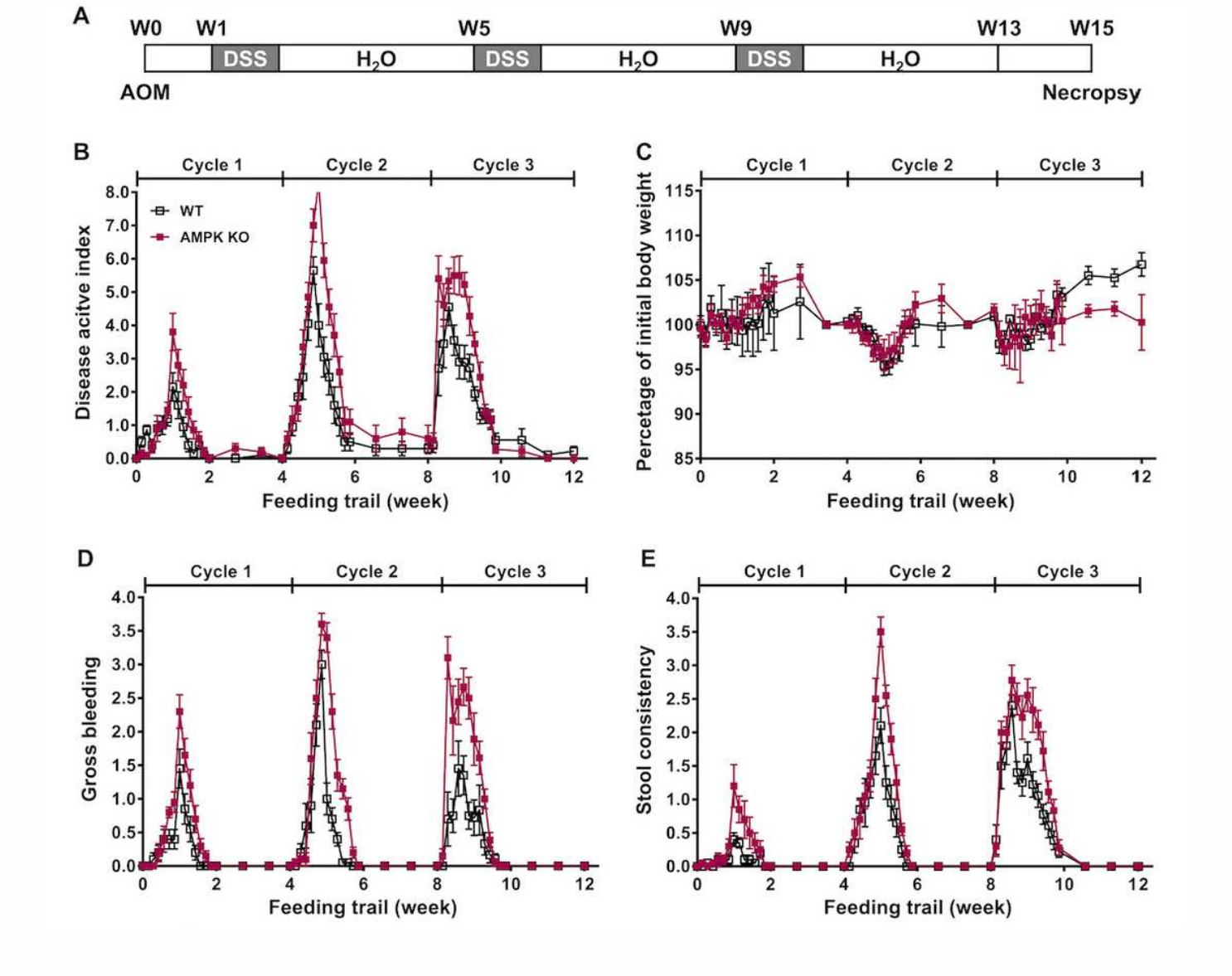

Figure 3

AMPK ablation aggravates disease activity in an AOM/DSS-induced CRC mouse. (a) Experimental design of azoxymethane (AOM) and dextran sulfate sodium (DSS) induced colorectal cancer. Wild-type (WT) and AMPK intestinal stem cell-specific knockout (AMPK KO) mice at the age of 15 weeks were injected with AOM (10 mg/kg body weight) at the first day of experimental week 0 (W0). One-week after AOM injection, mice were subjected to 3 cycles of DSS induction. In each cycle, 1.0 % (w/v) DSS was provided in drinking water for 7 days followed by a 3-week of recovery. (b) Disease activity index over time, which is the sum of body weight loss (c), fecal gross bleeding (d), and stool consistency (e). Mean ± SEM, n = 9.

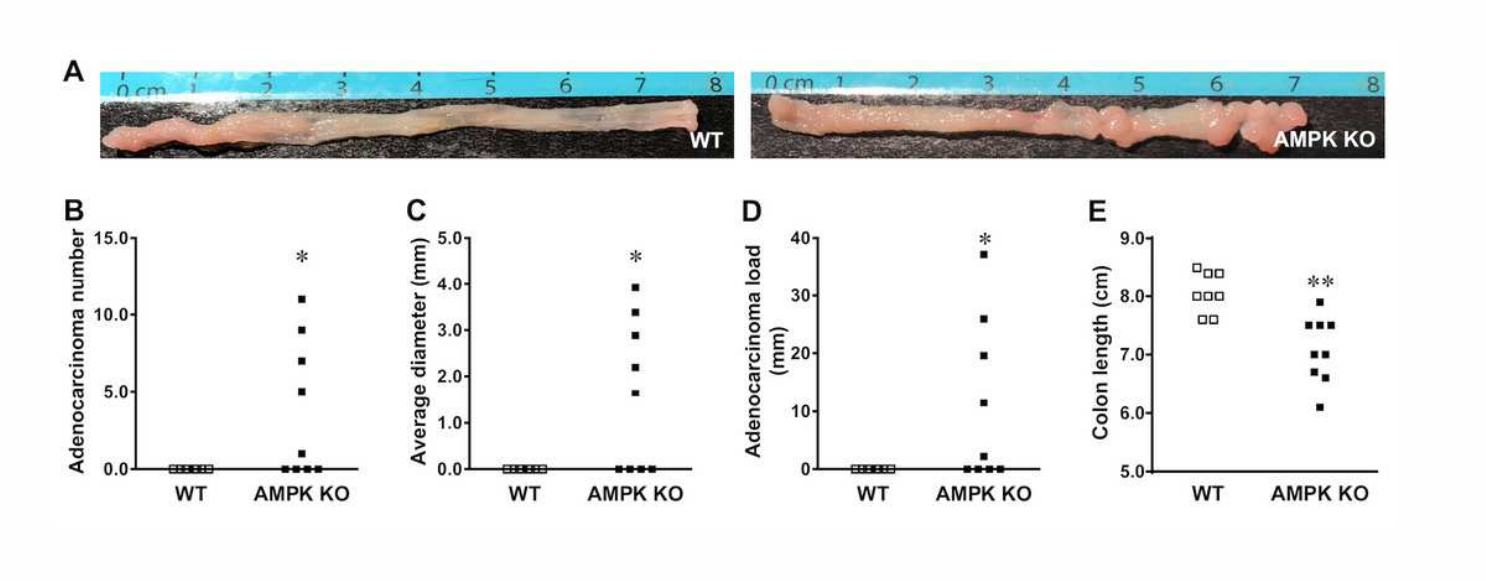

Figure 4

AMPK knockout accelerates adenomatous polyp development in an AOM/DSS- induced mouse. Wild-type (WT, □) and AMPK intestinal stem cell-specific knockout (AMPK KO, ■) mice were induced colon tumor with azoxymethane and dextran sulfate sodium and euthanized at the age of 30 weeks. (a) The representative images of the longitudinally opened colon. (b) Adenomatous polyp number. (c) Average adenomatous polyp diameter. (d) Adenomatous polyp load per mouse. (e) Colon length. Mean ± SEM, n = 9, *: $P < 0.05$; **: $P < 0.01$.

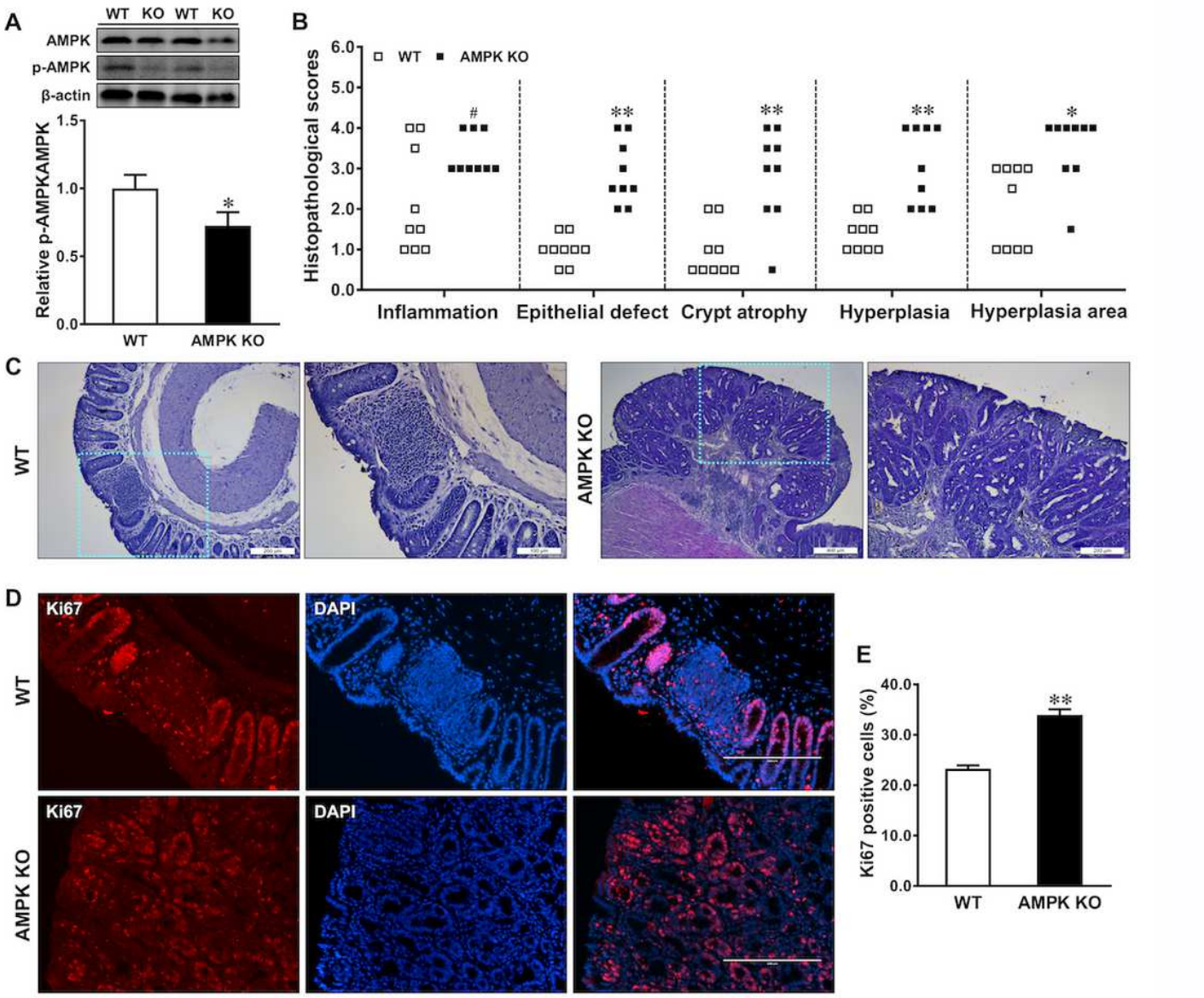

Figure 5

AMPK deficiency accelerates colorectal tumorigenesis. Wild-type (WT, □) and AMPK intestinal stem cell-specific knockout (AMPK KO, ■) mice were induced colon tumorigenesis with azoxymethane and dextran sulfate sodium and euthanized at the age of 30 weeks. (a) Relative p-AMPK/AMPK in colonic tissue. (b) Histopathological scores of colonic tissues. (c) Representative hematoxylin and eosin staining of distal colonic tissues; the blue rectangle highlighted the area was enlarged in the right image. (d) Representative immunofluorescent staining images of Ki67 (red) and DAPI (blue) of the frozen colonic tissue section. Ki67 positive staining represents proliferating cells. Scale bars are 200 μm. (e) The percentage of Ki67-positive nuclei out of the total nuclei was counted using Image J. Mean ± SEM, n = 9, #: $P < 0.1$; *: $P < 0.05$; **: $P < 0.01$.

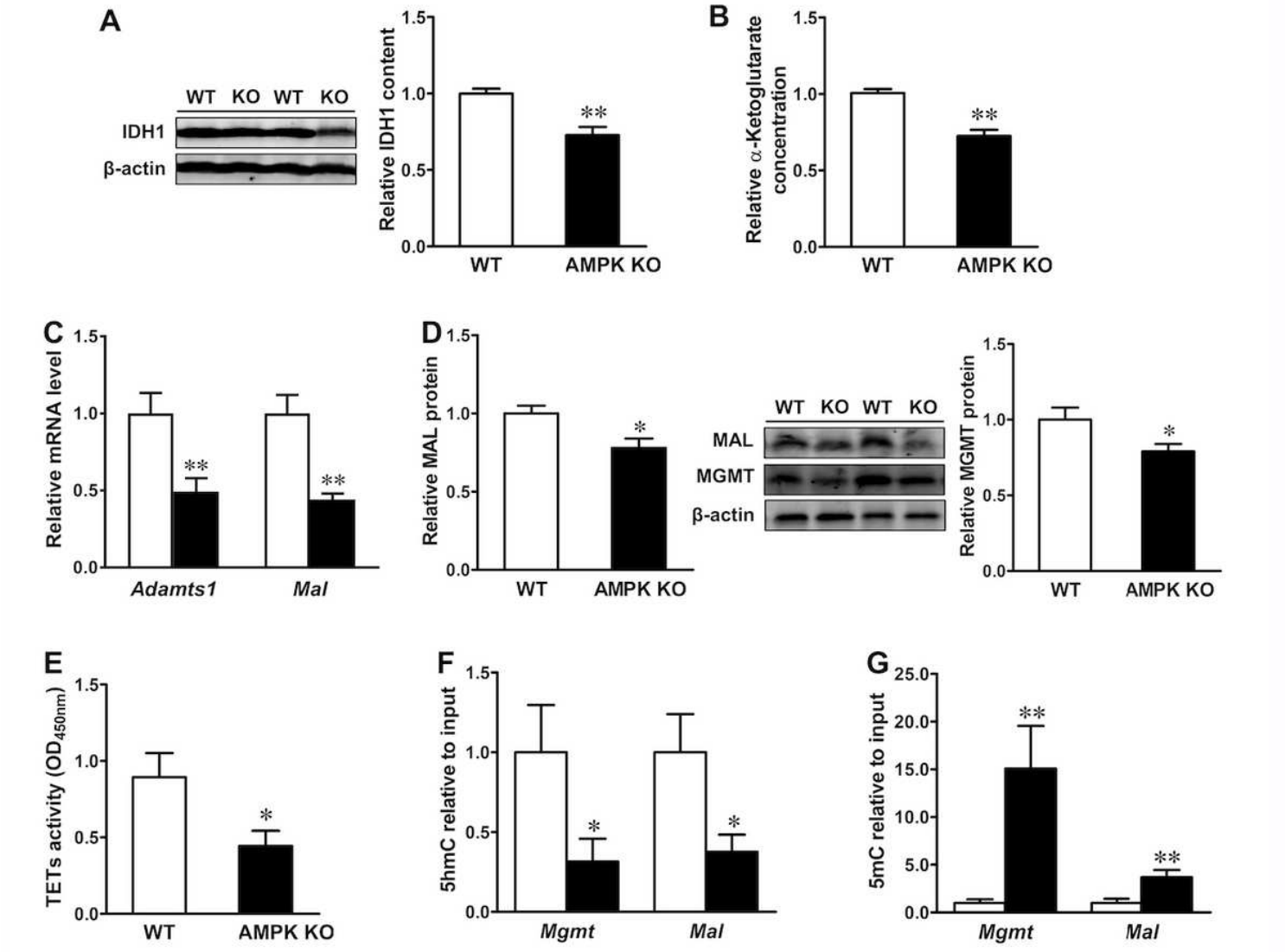

Figure 6

AMPK ablation inhibits colonic α-Ketoglutarate contents and TETs activity in AOM/DSS-induced mice. Wild-type (WT, □) and AMPK intestinal stem cell-specific knockout (AMPK KO, □) mice induced colon tumors with azoxymethane and dextran sulfate sodium and euthanized at the age of 30 weeks. (a) Relative protein contents of IDH1 in colonic tissue. (b) Relative α-Ketoglutarate concentration. (c) The mRNA expression of Adamts1 and Mal. (d) Relative protein contents of MAL and MGMT in colonic tissue. (e) The activity of ten-eleven translocation hydroxylases (TETs). (f) 5hmC and (g) 5mC modifications in the promoters of Mgmt and Mal. Mean ± SEM, n = 9, *: P < 0.05; **: P < 0.01.

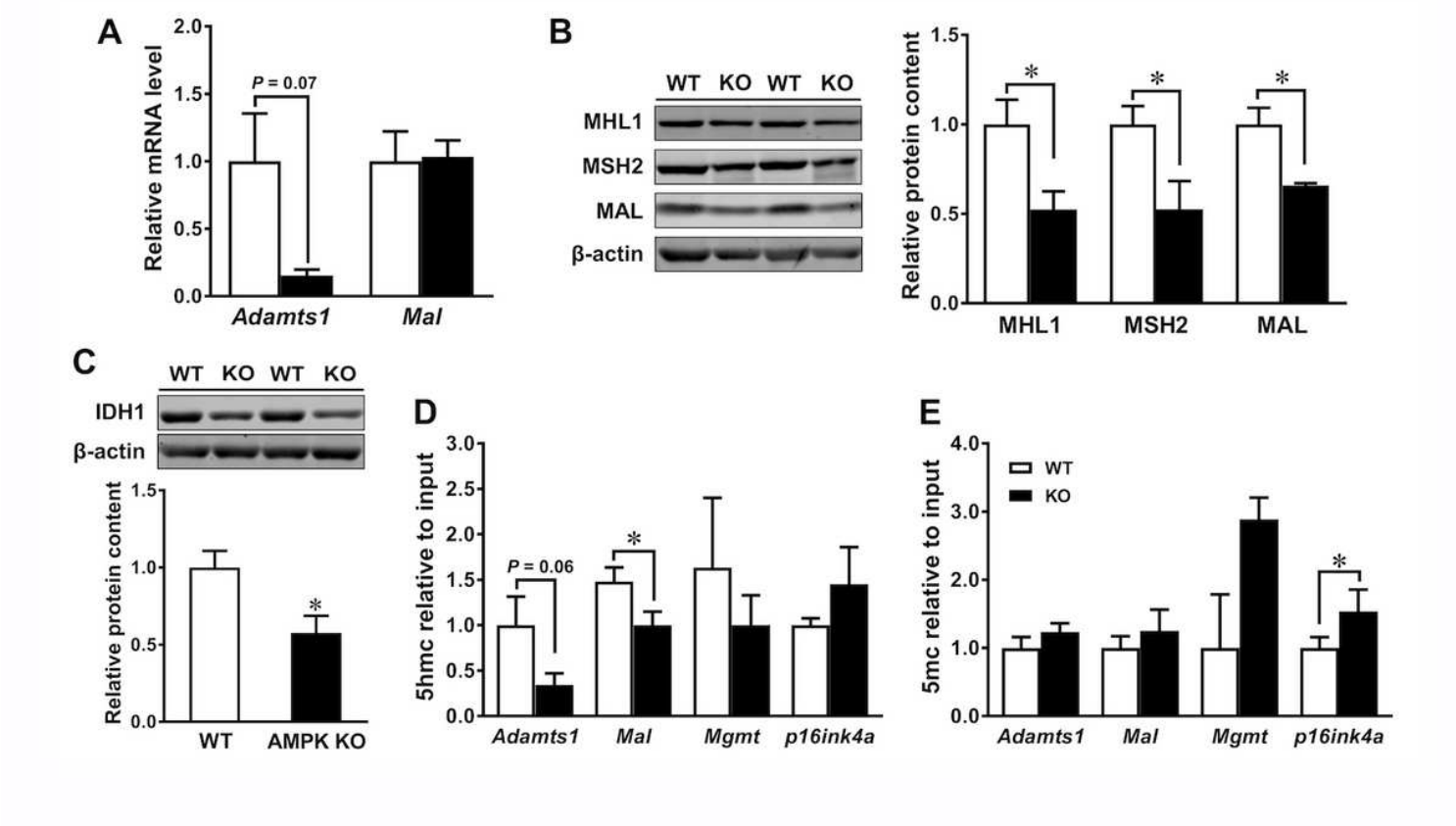

Figure 7

AMPK prevents promoters hypermethylation in Caco-2 cell. □: Caco-2 cells were transfected with eGFP plasmid(WT); □: Caco-2 cells were transfected with pAMPKα K45R plasmid (AMPK KO). (a) The mRNA expression of Adamts1 and Mal. (b) Relative protein contents of MLH1, MSH2 and MAL. (c) Relative protein contents of IDH1. (d) 5hmC and (e) 5mC modifications in the promoters of Adamst1, Mal, Mgmt and p16ink4a. Mean ± SEM, n = 3, *: P < 0.05.

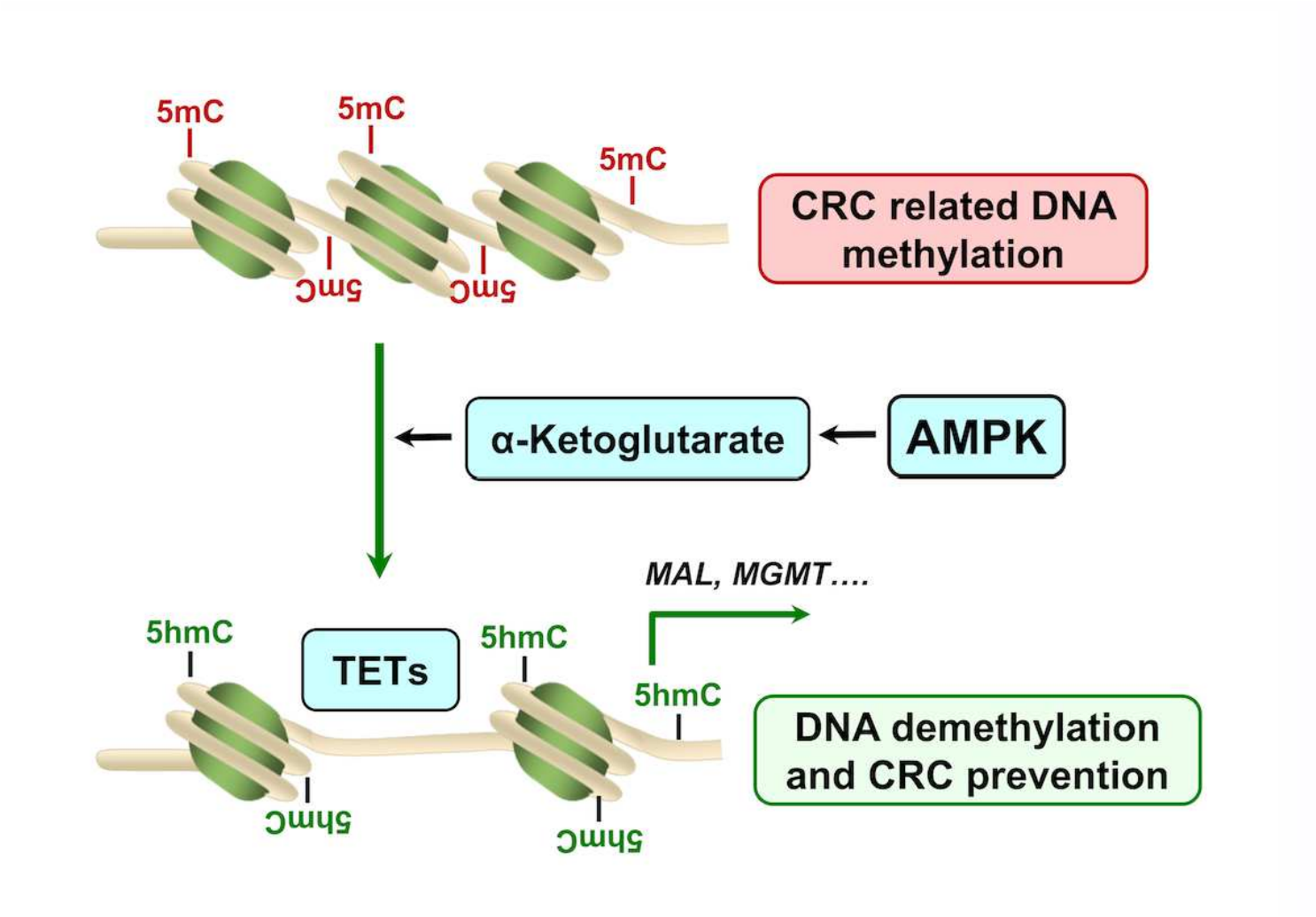

Figure 8

Schematic diagram of mechanisms linking AMPK to epigenetic modifications of colorectal tumorigenesis. In an AOM/DSS induced-CRC mouse model, AMPK activation increases α-Ketoglutarate, which promotes TET-mediated DNA demethylation in the promoters of antioncogenic genes, suppressing/preventing colorectal carcinogenesis. AMPK: AMP-activated protein kinase; CRC: colorectal cancer; Mal: myelin and lymphocyte; Mgmt: O-6-methylguanine-DNA methyltransferase promotor regions; TETs: ten-eleven translocation hydroxylases